Potential benefits from Thermosyphon-PCM (TP) integrated design for buildings applications in Toronto

M.E. Poulad[1], and Alan Fung[2]
[1]PhD candidate, Mechanical and Industrial Engineering (MIE) Department, RU, Toronto, ON
[2]Associate Professor, MIE Department, Ryerson University (RU), Toronto, Ontario, Canada

Abstract

The integration of phase change material (PCM) and thermosyphon is introduced as a mean to transfer solar radiation into the indoor air. A steady state, one dimensional model is analysed here to investigate the potential benefits of the TP.

Analysis of the power transferred by the thermosyphon-PCM panel shows that more than one mega-watt-hour per square meter (MWh/m^2) energy can be transferred into buildings in Toronto annually. Therefore, by mounting TP, which has thermal resistance on an order of -4 K/W, solar energy can be a source of heating for buildings. In the coldest month of the year, January, the insolated surface of the TP can reach as high as 54.5°C.

1 Introduction

In the 20th Century many buildings became totally dependent on fossil fuel energy to make them habitable. Performance of a building envelope could be enhanced by a well-designed thermo-diode panel (TDP) (Varga et al. 2002). Such a system could provide a means to achieve a cost effective Net Zero Energy Building (NZEB) in a cold climate like Canada. This overall investigation will address the fact that 63% of Canadian residential energy goes to space heating (Natural Resources Canada 2009). This paper illustrates the conceptual design and simulation of a cladding material incorporated with thermosyphon, which is suitable for use in new and existing buildings. Such a panel is capable of acting as a TDP. i.e., it has a low thermal resistance in the forward direction and a low thermal conductivity in the reverse direction. TDP has potential application in buildings to transfer thermal energy from incident solar radiation and conduct it through the panel to the interior in the heating season. It also acts as an insulating material and reduces heat loss when the building interior is at a higher temperature than the outdoor temperature. When such a panel was added to the south-facing wall of a building in Los Alamos, New Mexico, it led to 50% of the incident solar radiation being used for heating purposes during the winter (Varga et al. 2002). Other simulation results and experimentations revealed that at least 40% of solar radiation energy could be transferred to the building envelope (Chun et al. 2009).

A two-phase closed thermosyphon is a simple but effective heat transfer device (Chen et al. 2002; Dunn & Reay 1994; Esen & Esen 2005; Tundee et al. 2010; Imura et al. 2005). It is an evacuated closed pipe with a liquid pool at the bottom (Figure 1). It is best described by its three sections: condenser with length of L_c, adiabatic with length of L_a, and evaporator with length of L_e. Heat is input through the evaporator section where the liquid pool exists, turning the saturated working fluid into a vapour. The vapour rises and passes through the adiabatic section to the condenser section, where the vapour condenses and gives up its latent heat of evaporation (h_{lv}). The condensate falls back to the evaporator section by gravity. The selection of the working fluid for the thermosyphon involves the thermal characteristics of the

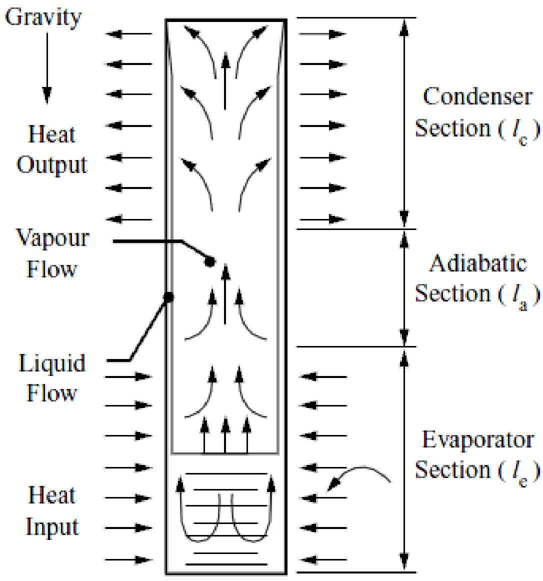

Figure 1: Conventional thermosyphon structure (Joudi and Witwit 2000)

fluid, environmental factors, the desired lifetime of the heat pipe and compatibility with the material of the heat pipe container.

There are several available working fluids to choose from. In this short analysis the working fluid selection is based on the widely used parameter called Merit number. Basically fluids that have high latent heat and surface tension tend to have a higher Merit number. Conveniently, merit number (M') is defined as a criterion to select the working fluid; the higher M'means better quality. Water has the maximum merit number amongst all candidates as potential fluid for heat pipe/thermosyphon manufacturing. Merit number is defined as (Faghri 1995):

$$\boldsymbol{M'} = (\frac{h_{lv}k_l^3 s_l}{\mu_l})^{1/4} \tag{1}$$

Where subscript l and v stand for liquid/fluid and gas/vapour, respectively, inside the thermosyphon, h is the latent heat of evaporation (lv represents liquid to vapor phase change), k, s, and μ are thermal conductivity, surface tension, and dynamic/absolute viscosity of the liquid, respectively. As surface tension is not an issue in the thermosyphon (condensed fluid returns back to the evaporator by gravity not by capillary pressure), the above index is an important for heat pipe design. Another index has yet to be specifically defined for the thermosyphon. The amount of fluid inside the thermosyphon should be experimentally optimised. Generally, from the classical Nusselt theory, the total volume of the fluid (V) was determined as Equations (2) to (5) (Faghri 1995). It is assumed that the thermosyphon is in steady state conditions (i.e., a constant temperature difference between the wall and the saturated vapour in condenser, $T_{sat} - T_{w,c}$, and a constant temperature difference between saturated vapour and the part of evaporator which is covered by the liquid film, $(T_{w,f} - T_{sat})$. Figure 2 illustrates a wall section of the thermosyphon and all the parameters used in Equations (2) to (5).

$$V = V_f + V_p \tag{2}$$

$$V_p = \frac{\pi D^2}{4} L_p \tag{3}$$

$$\boldsymbol{V_f = \pi D(\frac{4k\mu_l}{\rho_l^2 g h_{lv}})^{\frac{1}{4}}[(T_{sat} - T_{w,c})^{\frac{1}{4}}\left(\frac{4}{5}L_c^{\frac{5}{4}} + L_a L_c^{\frac{1}{4}}\right) + \frac{4}{5}(T_{w,e} - T_{sat})^{1/4}(L_f{}^{5/4} - L_{fp}{}^{5/4})]} \tag{4}$$

$$\boldsymbol{L_p = L_e - L_c\left(\frac{T_{sat}-T_{w,c}}{T_{w,e}-T_{sat}}\right) + [\frac{1}{4k(T_{w,e}-T_p)}](\frac{\mu_l}{\rho_l^2 g h_{lv}})^{1/3}(\frac{3Q_p}{\pi D})^{4/3}} \tag{5}$$

In the above equations, D is the internal diameter, h_{lv} is the latent heat of evaporation, subscript l refers to liquid phase property (this script is used for density, ρ, and dynamic viscosity, μ), k is the thermal conductivity of the working fluid, and g is the gravitational acceleration.

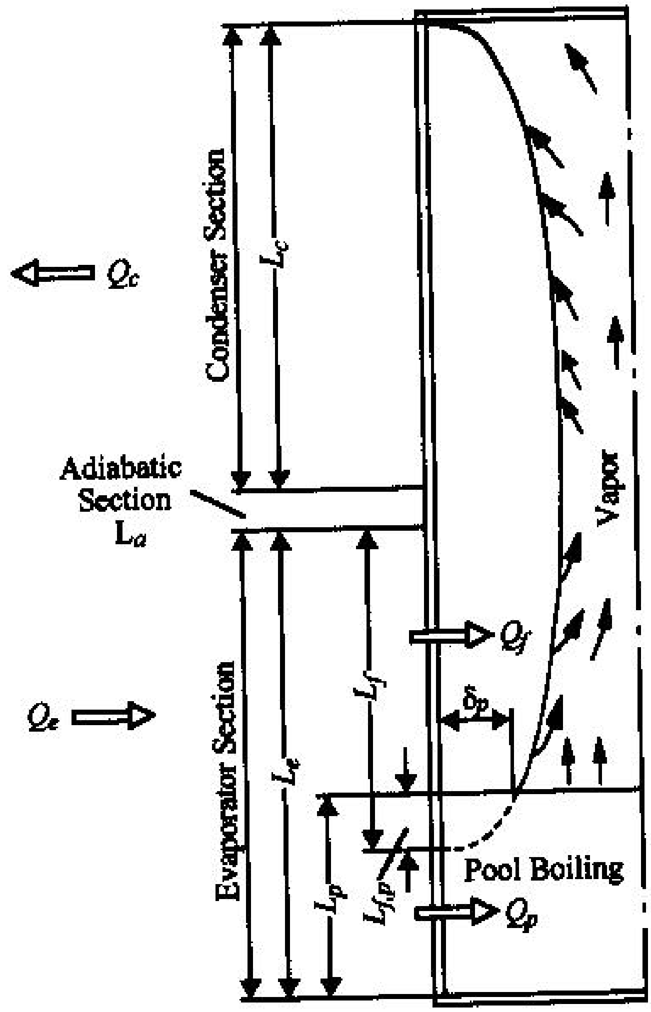

Figure 2: Thermal fluid model of condensation and evaporator (Faghri 1995)

Table 1 presents some operating characteristics of a thermosyphon. In this project, copper container and water are selected as the thermosyphon body and working fluid inside, respectively.

It is interesting that the thermosyphon has no macro scale moving parts and is considered fully passive (Singh et al. 2011). In addition, phase change material (PCM) is well known as a sustainable source of thermal storage. PCM can be charged and discharged without reducing its power to store energy (Gracia et al. 2010). The combination of these two identities provides a panel that can be integrated with the south facing wall by storing the solar energy (charge). The storage comprises an energy storage container, full of PCM, and a two-phase closed thermosyphon loop. Cold water is heated during discharge by passing through the charged PCM. The thermosyphon loop is filled with an adequate amount of water as working fluid. The adequacy of the amount of fluid is discussed in some references (Faghri 1995; Zohuri 2011; Bezrodnyi & Alekseenko 1977 ; El-Genk & Saber 1999).

Table 1: Typical Operating Characteristics of Thermosyphons (Zohuri 2011)

Temperature Range (°C)	Working Fluid	Container Material	Axial Heat Flux (kW/cm^2)	Surface Heat Flux (kW/cm^2)	Merit Number (M')
-45 to 120	Methanol (CH_3OH)	Copper, nickel, stainless steel	0.45 at 10°C	75.5 at 100°C	25.6 at 50°C
5 to 230	Water (H_2O)	Copper, nickel	0.67 at 200°C	146 at 170°C	97.8 at 60°C

Phase Change Material (PCM) Storage

The phase change process either releases or absorbs heat. Most natural PCMs transform from liquid to solid or vice versa. They can be either organic or inorganic. Solid-solid PCM is also, artificially, developed to mix with building materials, such as gypsum and concrete (Whitman et al. 2011).

Latent heat storage is an efficient way of storing thermal energy due to two key factors. First, latent heat storage using PCMs has a much higher storage density than sensible heat storage. Second, in using the latent heat storage method there are fewer temperature fluctuations, and a smaller temperature difference between storing and releasing heat compared to sensible heat storage (Farid et al. 2004). In one recent study, it was found that the storage time of hot water, the produced hot water mass and total heat accumulated in the solar water-heating system having a heat storage tank combined with PCMs were 2.59 - 3.45 times that of the conventional solar water-heating system without PCMs. This translates directly into a cost savings as a smaller tank with less insulation could be used in conjunction with PCM storage (Canbazoglu et al. 2005). Several materials have been investigated to understand their applicability to solar thermal applications. Issues such as the degradation of thermal properties, phase segregation, and stability have been researched to ensure good systemic performance (Farid et al. 2004). Current research indicates that PCMs such as salt hydrates, paraffin (e.g., RT58), and fatty acids are potential candidates for thermal storage in solar applications (Canbazoglu et al. 2005). More specifically, fatty acids including capric, lauric, palmitic, and stearic acids possess good thermal characteristics making them promising PCMs for solar applications (Farid et al. 2004). Fatty acids, with a melting range between 30 and 65 ºC and latent heat of fusion varying from 153 to 180 kJ/kg, could potentially be used in space and domestic hot water applications, as they have demonstrated good thermal stability in terms of thermal cycling when used as latent heat storage materials in solar thermal applications (Sari 2003).

Developing and using a PCM involves the understanding of three essential subjects: container materials, heat exchangers and PCMs themselves. There are two available PCMs that can be considered for the proposed system: Polyglycol (E600) with melting point of 22°C and eutectic mixture of myristic acid (MA) and stearic acid (SA) with melting point of 44.13°C makes a good combination with thermosyphon to store solar energy.

2 Methodology

The simulation should answer the feasibility of the design in Toronto weather conditions.

Figure 3 shows the sketch of the design. To analyse the evaporator surface temperature, which is exposed to the solar radiation, one dimensional energy balance is employed, see Figure 4.

Equations are derived based on the first law of thermodynamics as follows:

$$\alpha A q_{Solar} = q_{in} A_{hp} + (q_{con} + q_{rad}) A \tag{6}$$

where: Q=qA, A is the radiated area, q_{Solar} is the solar radiation to the surface, $A_{hp}$is the thermosyphon cross section area, $q_{in}$is the power transmitted to the building envelope through the condenser of the thermosyphon, $q_{con}$is the convection power loss due to the wind outside, α is the surface absorptivity, and q_{rad} is the net radiation power loss to the surroundings due to the surface and sky temperatures ($\varepsilon\sigma(T^4 - T_\infty{}^4)$). All heat flux (q) units are in watt per square meter (W/m^2).

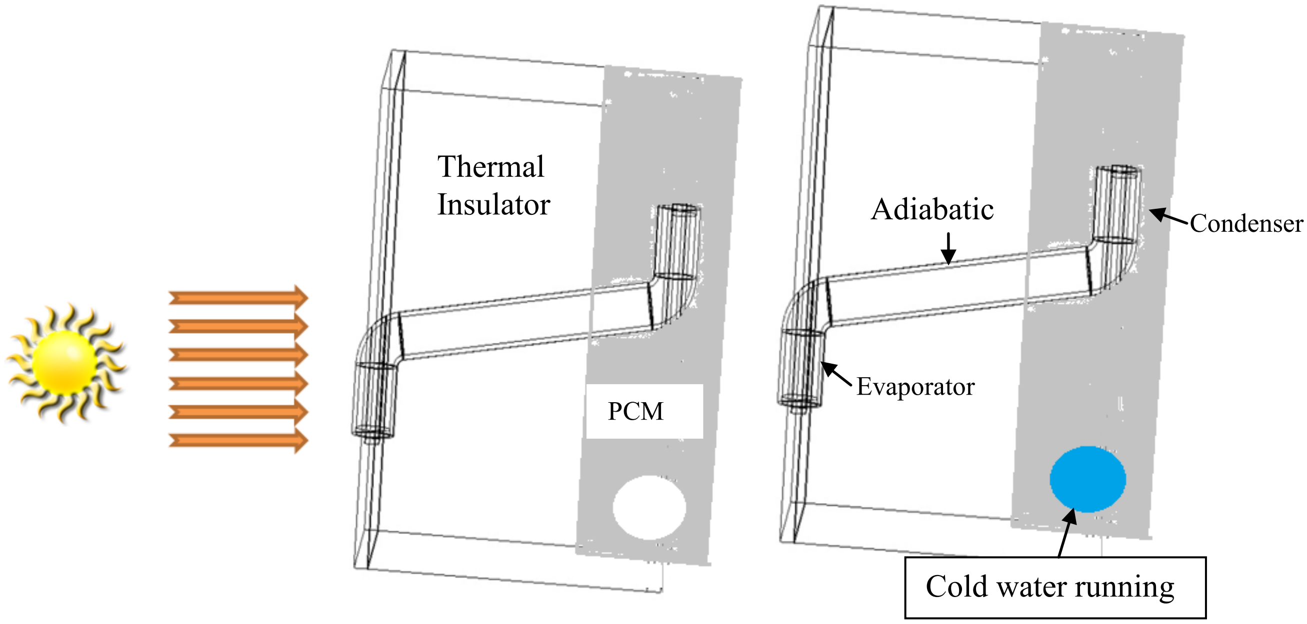

Figure 3: PCM-thermosyphon combination in charging (left) and discharging (right) conditions

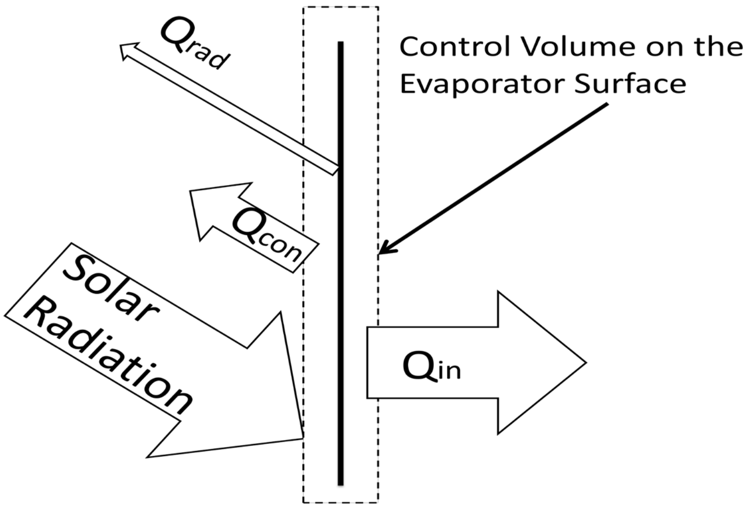

Figure 4: Energy balance for control volume on the evaporator surface

As Equation (6) implies, to maximise the Q_{in}, the other terms in the right side of the equation should be minimised. Therefore, it is important to cover the evaporator surface with a transparent material (e.g., Plexiglas) in order to reduce outside convection heat transfer. Based on the Equation (6), the steady state governing equation for calculating the surface temperature (T) would be:

$$A\alpha q_{solar} = Q_{in} + \left[\bar{h}_o(T - T_{air}) + \varepsilon\sigma\left(T^4 - {T_\infty}^4\right)\right]A \quad (7)$$

where: α and ε are solar absorptivity and emissivity, respectively, of the surface under investigation, σ is Stephen-Boltzmann constant (5.67 x10^{-8} W/m^{2}K^4), T_∞ is sky temperature (K), T_{air} is air temperature (K) (this is close to the T_∞), T is the surface temperature (K), $\bar{h}_o$ is convective heat transfer coefficient (W/m^{2}K), and A is the exposed surface to radiation (m^2).

To calculate Q_{in}, the thermal resistance of the panel (Figure 2) should be estimated. Figure 4 shows the physical shape or geometry (top) and the thermal resistant network (bottom) of the problem. Arrows point from the relevant surfaces of the geometry to their corresponding temperatures in the network. Thickness of each layer is noted on top of the geometry. G, 10 cm, and H, 20 cm, are the width and height of the panel (i.e., the surface area whose temperature is under investigation is GH).

Recalling the notations in Figures 5 and 2, the resistances (R_1 to R_7) are calculated as follows:

$$R_1 = \frac{t_1}{k_1(GH - A_p)} \quad (8)$$

$$R_2 = \frac{t_2}{k_2(GH - A_p)} \quad (9)$$

$$R_3 = \frac{t_3}{k_3(GH - A_p)} \quad (10)$$

$$R_4 = \frac{t_4}{k_4(GH - A_p)} \quad (11)$$

$$R_7 = \frac{t_5}{k_5 GH} \quad (12)$$

$$R_5 = \frac{G}{6k_1 t_1 L_e} \quad (13)$$

$$R_6 = \frac{(1 + e^{\sqrt{B}G})G\sqrt{B} - 2(e^{G\sqrt{B}} - 1)}{L_c t_3 k_3 G\sqrt{B}(e^{G\sqrt{B}} - 1)} \quad (14)$$

where

$$B = \frac{k_4}{t_3 t_4 k_3} \quad (15)$$

$$R_{hp} = \frac{ln\frac{r_o}{r_i}}{2\pi k_{Cu}}\left(\frac{1}{L_c} + \frac{1}{L_e}\right) + \frac{\pi r_o^2 T_v F_v\left(\frac{L_e}{6} + L_a + \frac{L_c}{6}\right)}{\rho_v h_{lv}} \quad (16)$$

$$F_v = \frac{8\mu_v}{\rho_v h_{lv} r_{h,v}^2 A_v} \quad (17)$$

where F_v is frictional coefficient for circular vapour-flow passage (Chi 1976), subscript v refers to vapour phase, $r_{h,v}$ is hydraulic radius of vapour ($\approx r_i$), r_i, r_o, and A_{hp} are the internal and external radius, and cross section area of the thermosyphon, respectively, L_e, L_a, L_c are evaporator, adiabatic and condenser length, respectively, α is the angle between the adiabatic section of the thermosyphon and horizon. Considering uniform temperature for walls and inside air (T_{in}), the total thermal resistance between investigating surface and the inside zone would be:

$$\sum \mathrm{R} = \frac{(R_5 + R_{hp} + R_6)(R_1 + R_2 + R_3)}{(R_5 + R_{hp} + R_6) + (R_1 + R_2 + R_3)} + \frac{1}{GH(h_{ri} + h_i)} + R_4 + R_7 \quad (18)$$

where:

$\bar{h}_{ri} = \varepsilon\sigma(T_0^2 + T_{in}^2)(T_0 + T_{in})$ and $\bar{h}_{ro} = \varepsilon\sigma(T^2 + T_{air}^2)(T + T_{air})$

Now, Equation (7) can be solved for T by substituting Q_{in} as follows:

$$Q_{in} = \frac{T - T_{in}}{\sum \mathrm{R}} \quad (19)$$

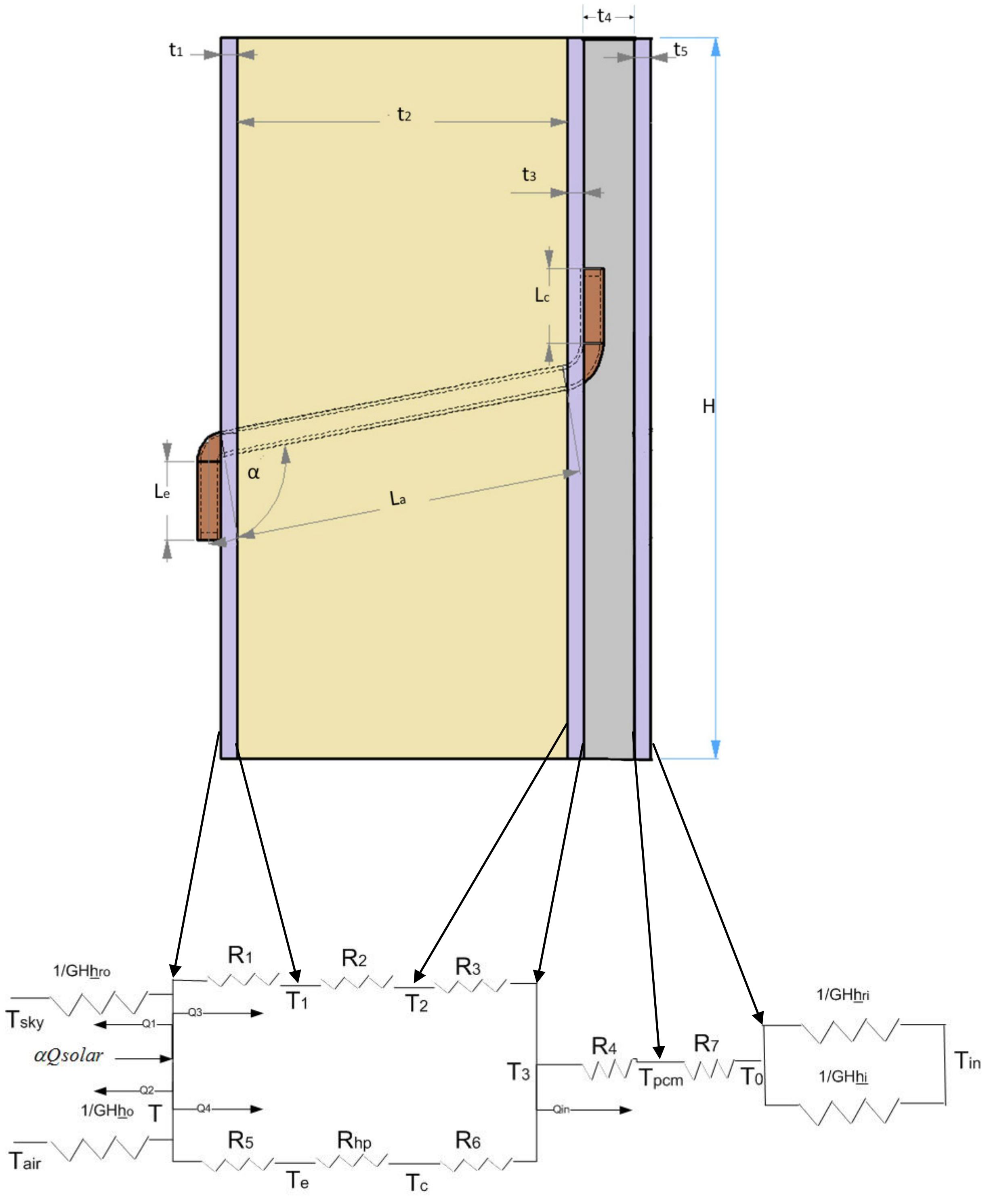

Figure 5: TP panel (top) and its thermal resistance network (bottom), related surfaces are connected by arrows. T and T_3 represent the average temperature of the surfaces

Assuming the interior temperature, $\bar{h}_i$ and $\bar{h}_o$ as 20℃, 2 W/m^{2}K and 20 W/m^{2}K, respectively, simulation of the hot end surface of the thermosyphon can be estimated in Toronto. The outdoor convective heat transfer coefficient ($\bar{h}_o$) is estimated based on average air speed (Khalifa & Marshall 1990). As is known from information taken from The Weather Network website[1], the lowest daily average low ambient temperature is about -7℃ in January (the coldest month of the year); therefore, it is very important to get maximum possible heat from the Sun in this month. The surface temperature of the TDP is calculated in this month to investigate the potential energy that can be transferred into the building through the TP. Taking into account that the Sun is not always available, it is very important that TP not only is fast in transferring the solar energy (by using thermosyphon) but also stores heat for near future use (in the PCM).

3 Results

A MATLAB code is developed to calculate the surface temperature (T) by solving Equations (7) and (18). It takes Toronto weather conditions (e.g., T_∞ and q_{solar}) as an input and provides the T and Q_{in} on an hourly basis. The physical parameters are given based on the properties of pure aluminum for material with thickness t_1, t_3 and t_5, pure copper for the thermosyphon and urethane foam (two-part mixture) for thickness t_2. In addition, the width and height of the panel are considered as 10 cm and 30 cm respectively, and the inside and outside diameters of the pipe are 10mm and 12 mm respectively, with condenser, adiabatic and evaporator length of 10cm, 15cm and 10cm in turn. Table 2 presents the calculated values of some thermal resistances. As Equation (18) implies, $T_{in}$and T_0 affect the value of R. By fixing the difference between the temperatures ($T_0 - T_{in} = 10$), interior convective heat transfer ($\bar{h}_i$=*2W/m²K*), and changing the interior temperature (T_{in}) from 1°C to 20°C, the R-value changes from 17.001 K/W to 16. 243 K/W. The average value is reported in Table 2.

Table 2: Some thermal resistances (in K/W) in the TP panel

R_1	R_2	R_3	R_4	R_5	R_6	R_{hp}	R
0.00043	169.093	0.00014	8.953	0.234	2.801	0.00042	16.654

Aside from a 1 mm aluminum plate (R_3), the thermosyphon (R_{hp}) has the least thermal resistance (in order of -4). This causes the panel to transfer all the radiation heat through the thermosyphon and heat up the PCM as soon as the sun shines. The thermosyphon has three distinct thermal resistors the two ends (evaporator and condenser) with resistance of 0.000724 K/W at each end and vapour resistance in the middle of the pipe with $2.24\text{x}10^{-9}$ K/W resistance. This implies that thermal resistance of a thermosyphon is dependant on the quality of the surfaces and materials of both ends. The maximum thermal resistance goes to PCM (R_4), which is not really intended to transfer heat; it is intended to store the heat and the aluminum plate in contact with PCM (t_5), which conducts its heat to the indoor air.

The variation of power transferred and surface temperature in January in Toronto is shown in Figure 6. For this calculation, the temperature of the air around the surface is taken equal to the sky temperature of the outdoor (T_∞). In this month, 79.6 kWh/m^2 solar energy is released, whereas 213 Wh energy is transferred into the building. Recalling the property of the thermosyphon (thermo-diode), this is the net energy transfer into the building during the first month of the year. This condition (i.e., the sizes and type of materials) has yet to be optimised for the weather conditions in Toronto. Meanwhile, the calculations are based on typical available materials and thermosyphon, which is possible to manufacture from stock materials. The values are calculated based on the worst case scenario (i.e., continuous heat loss due to the convection on the surface, and inside temperature in assumed 20°C). Practically, the convection can be substantially reduced by covering the surface with a transparent material

[1] The sampling period for this data covers 30 years. Record maximums and minimums are updated annually.

(e.g., Plexiglas). As is seen from Figure 6--assuming that the interior temperature is 20°C--as soon as the surface temperature is above 20°C, heat flows inside. The temperature of the surface reaches as high as 54.5°C in the coldest month of the year. This value increases to 83°C during the year.

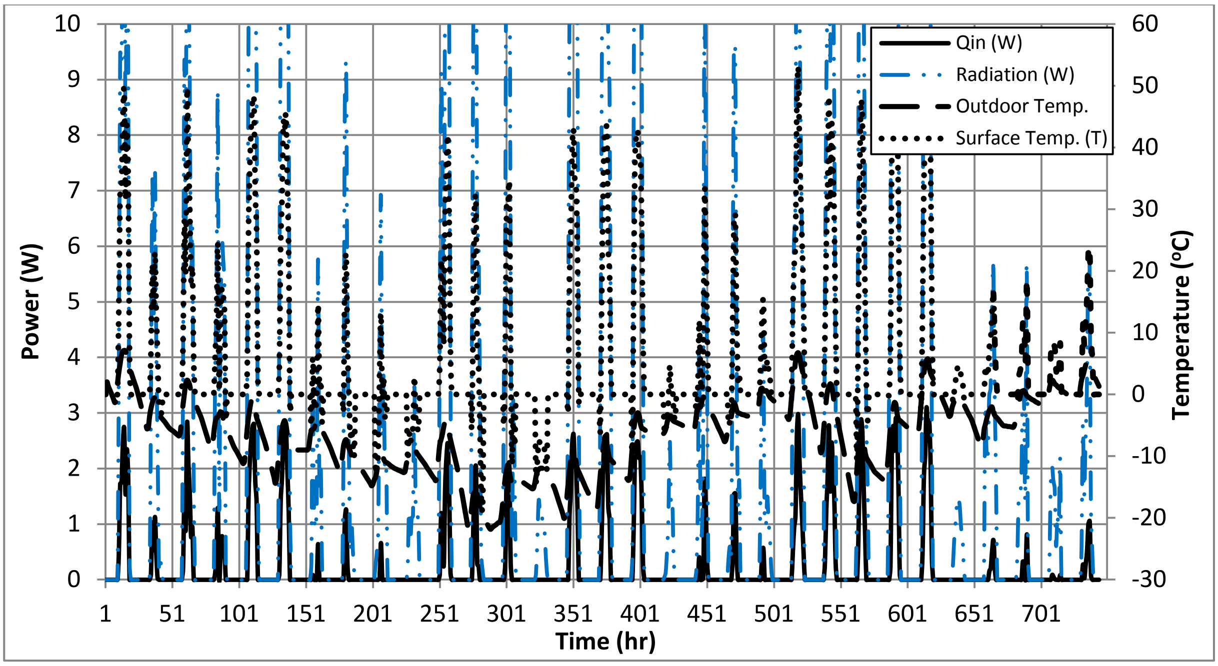

Figure 6: Maximum power that can be transferred (Q_{in}), radiation power, surface and outdoor temperatures in Toronto in January

The input file is source of information for most of the energy simulators (e.g., TRNSYS). Facts given in Table 3 are taken from the input file. It depicts that, on the average, more than one mega-watt-hour per square meter (MWh/m^2) thermal energy can be harvested from the Sun.

Table 3: Annual (8760 hours) solar radiation facts in Toronto

Component	Fact
Average air temperature when the Sun shines (°C)	11
Average solar radiation (W/m^2)	231
Maximum solar radiation (W/m^2)	927
Number of hours the sun shines per year (50% of the year)	4375

Design parameters

To obtain the maximum benefit from TP, the following factors should be selected properly:

- **PCM melting temperature (T_m):** To reduce the interior temperature fluctuation, the PCM melting temperature should be inside the comfortable temperature range (i.e., 21°C to 24°C). Thus, Polyglycol E600 (Farid et al. 2004) is a good option with melting temperature of 22°C.
- **Overheating:** During the summer months, there are some hours when indoor temperature is above the set point (i.e., 24°C) and solar energy is transferred to the PCM, while all the PCM is melted. At this moment, the TP system should be equipped with sensors that flow the tap water into the TP to transfer the

heat from the PCM into a domestic hot water (DHW) tank (see right side of Figure 3, discharge condition).

- **Fluid type:** The fluid should be selected based on an estimation of the outside temperature range and its Merit number. Water is a good option with a working temperature range of 5°C to 230°C and Merit number of 25.6 at 50°C.
- **Fluid filling:** Generally, from the classical Nusselt theory, the minimum volume of the fluid (V) can be determined (Faghri 1995). As a rough estimation, it is advised that the fluid volume obey the following rule (Bezrodnyi & Alekseenko 1977):

  $$V > 0.001D(L_e + L_a + L_c) \quad (20)$$

  where D is the internal diameter of the thermosyphon tube. This equation provides a film thickness of more than 0.3 mm over the total length of the inner surface of the thermosyphon. Although Equation (20) provides a criterion for minimum filling of fluid, the optimum value is estimated experimentally (Wright 1984). Engineering Sciences Data Unit (ESDU) suggests 40% to 60% of the evaporator volume should be filled with the fluid (Chisholm, et al. 1983).
- **Thermal volume change of the PCM:** expansion and contraction of the PCM during phase change should be calculated and enough space should be provided for them.

Heat transfer limitations in thermosyphon

Heat transfer increases across the thermosyphon by increasing the temperature difference at both ends until it reaches to a maximum value. This maximum value may be due to:

- **Vapour pressure limit:** as operating pressure inside the thermosyphon, for this design, is about 0.1 atmosphere (water boils around 40°C at this pressure), the pressure drop of the vapour may be significant compared with the pressure in the evaporator. An estimation of the vapour pressure limit is given in the ESDU.
- **Sonic limit:** when operating pressure is low, the vapour velocity may be high compared with sonic velocity in the vapour. An estimation of the sonic limit is given in the ESDU. This limit is 7.8 MW/m^2 for water at 20°C, while it increases to 277 MW/m^2 at 100°C.
- **Dryout limit:** this limit addresses the amount of fluid. In a vertical thermosyphon, Dryout is avoided if the filling meets the conditions called for in “Fluid filling” section above.
- **Boiling limit:** this limit occurs between the fluid and heated wall of the evaporator when a stable film of vapour is formed in this region. If the ratio of the length to the internal diameter of the evaporator exceed 10 ($L_e/D>10$) and the working temperature is 20°C, or 68 ($L_e/D>68$) while the working temperature is 100°C, the sonic limit occurs before boiling limit.
- **Flooding limit:** this limit is sometimes called “entrainment” or “counter-current flow”. When there is enough fluid to prevent dryout happening, the fluid may be entrained by vapour to flow back (downward) to the evaporator after condensing on the condenser surface. This limits the maximum axial vapour mass flux in a vertically operated thermosyphon as (Chisholm, et al. 1983):

$$\frac{Q_{max}}{Ah_{lv}} = f_1 f_2 \rho_v^{0.5}[g(\rho_l - \rho_v)\sigma]^{0.25} \quad (21)$$

Where A and h_{lv} are the cross section area and latent heat of evaporation of the fluid respectively, and $f_1$is a function of the Bond number (Bo), which is defined as:

$$Bo = D[g(\rho_l - \rho_v)/\sigma]^{0.5} \quad (22)$$

The value of f_2 is a function of the dimensionless pressure, K_p, which is defined as:

$$K_p = \frac{p_v}{[g(\rho_l - \rho_v)\sigma]^{0.5}} \quad (23)$$

and

$$f_2 = \begin{cases} K_p^{-0.17} \; if \; K_p \leq 10^4 \\ 0.165 \; if \; K_p > 10^4 \end{cases} \quad (24)$$

In this TP, where Bo number is about 8, the ESDU suggests the f_1 value of 7.6 and f_2 is calculated based on Equations (23) and (24), which is 0.51.

Amongst the above limitations, whichever that gives the lowest value should be considered as maximum heat flux of the thermosyphon. The ESDU recommends that the thermosyphon be designed to operate at less than 50% of the maximum heat flux.

4 Conclusions

A typical TP is designed to transfer solar energy directly into the indoor air in Toronto. It is estimated that up to one mega-watt-hour (MWh) of energy be taken from each square meter of the TP from the sun for heating buildings in Toronto annually. The surface temperature of the TP can be as high as 83℃, which proves the potential of flowing heat from the surface into the other side of the panel (either to heat up cold water for DHW tank in summer or to store energy into the PCM).

5 Future Work

This system is yet to be validated by experiment. Other parts of this project (e.g., producing a prototype, field testing) are in progress to validate the design. Additionally, the PCM is treated as lump with constant thermal properties; in future, transient conditions should be investigated for complete cycle of phase change. These are currently under investigation.

6 Acknowledgements

This work was funded in part by the NSERC Discovery Grant and the Smart Net-Zero Energy Building Research Network (SNEBRN).

7 References

Bezrodnyi, M.K., and D.B. Alekseenko. " Investigation of the critical region of heat and mass transfer in low temperature wickless heat pipes." *High Temp.*, 1977 : 15 309– 313.

Canbazoglu, Suat, Abdulmuttalip Sahinaslan, Ahmet Ekmekyapar, Go¨khan Y. Aksoya, and Akarsu, Fatih. "Enhancement of solar thermal energy storage performance using sodium thiosulfate pentahydrate of a conventional solar water-heating system." *Energy and Buildings*, 2005: 37 235–242.

Chen, B.-R., Y.-W. Chang, W.-S. Lee, and S.-L., Chen. "Long-term thermal performance of a two-phase thermosyphon solar water heater." *Solar Energy* , 1983: 83 (7), 1048–1055.

Chen, L., J. Gong, F. Sun, and C. Wu. "Effect of heat transfer on the performance of thermoelectric generators." *International Journal of Thermal Sciences*, 2002: 41 (1), 95–99.

Chi, S. W. *Heat Pipe Theory and Practice, A Sourcebook.* Washington: Hemisphere Publishing Co., 1976.

Chisholm, D., J.B. Goodacre, G. Rattclif, D.A. Reay, and G. Rice. *ESDU No. 81038, Heat pipes-performance of two-phase closed thermosyphons.* IHS, 1983.

Chun, W., Y.J. Ko, H.J. Lee, H. Han, J.T. Kim, and K. Chen. "Effects of working fluids on the performance of a bi-directional thermodiode for solar energy utilization in buildings." *Solar Energy*, 2009: 83 409–419.

Dunn, P.D., and D.A., Reay. *Heat Pipes, fourth ed.* Pergamon, 1994.

El-Genk, M.S., and H.H. Saber. "Determination of operation envelopes for closed\ two!phase thermosyphons." *International Journal of Heat and Mass Transfer*, 1999: 889-903.

Esen, M., and H., Esen. "Experimental investigation of a two-phase closed thermosyphon solar water heater." *Solar Energy*, 2005: 79 (5), 459–468.

Faghri, Amir. *Heat pipe science and technology.* Washington: Taylor & Francis, 1995.

Farid, M.M., A.M. Khudhair, A.K. Razack, and Said Al-Hallaj. "A review on phase change energy storage: materials and applications." *Energy Conversion and Management*, 2004: 45 1597-1615.

Gracia, Alvaro de, Lídia Rincón, Albert Castell, Melanie Jiménez, Dieter Boer, Marc Medrano, Luisa F. Cabeza. "Life cycle assessment of the inclusion of phase change materials (PCM) in experimental buildings." *Energy and Buildings*, 2010.

Imura, H., Y. Koito, M. Mochizuki, and H. Fujimura. " Start-up from the frozen state of two-phase thermosyphons." *Applied Thermal Engineering* , 2005: 25 (17–18), 2730–2739.

Joudi, K. A., and A. M. Witwit. "Improvements of gravity assisted wickless heat pipes." *Energy Conversion & Management* , 2000: 41 2041-2061.

Khalifa, A. J. N., and R. H. Marshall. "Validation of heat transfer coefficients on interior building surfaces using a real-sized indoor test cell." *International Journal of Heat and Mass Transfer*, 1990: Vol. 33 (10), 2219-2236.

Natural Resources Canada. 2009. http://oee.nrcan.gc.ca/english/index.cfm (accessed July 26, 2011).

Peterson, G.P. *An introduction to heat pipe: Modeling, Testing, and Applications.* New York: John Wiley & Sons, Inc., 1994.

Sari, Ahmet. "Thermal reliability test of some fatty acids as PCMs used for solar thermal latent heat storage applications." *Energy Conversion and Management* , 2003: 44 2277–2287.

Singh, Randeep, Sura Tundee, and Aliakbar Akbarzadeh. "Electric power generation from solar pond using combined thermosyphon and thermoelectric modules." *Solar Energy*, 2011: 85 371–378.

Tundee, S., P. Terdtoon, P. Sakulchangsatjatai, R. Singh, and A. Akbarzadeh. "Heat extraction from salinity-gradient solar ponds using heat pipe heat exchangers." *Solar Energy*, 2010: 84 (9), 1706–1716.

Varga, S., A. O. Oliveira, and C. F. Afonso. "Characterization of thermal diode panels for use in the cooling season in buildings." *Energy and Buildings*, 2002: 34, 227-235.

Whitman, C. A., M.B. Johnson, and M. A. White. "Characterization of Thermal Performance of a Solid-Solid Phase Change." *Thermochimica Acta*, 2011.

Wright, A. "Thermosyphons as heat transfer elements in large air pre-heaters." *Heat Recovery Systems* , 1984: Vol. 4, No. 4, 239-245.

Zohuri, Bahman. *Heat Pipe Design and Technology.* Boca Raton, FL: CDC Press, Taylor & Francis Group, 2011.

8 Nomenclature

A	Area
Bo	Bond number
D	Diameter
DHW	Domestic hot water
ESDU	Engineering science data unit
g	Gravitational acceleration
$\bar{h}$ & $\underline{h}$	Convective heat transfer coefficient
h	Enthalpy change due to phase change
HP	Heat Pipe/Thermosyphon
L & l	Length
M'	Merit number
MA	Myristic acid
MWh	Mega-watt-hour
NZEB	Net Zero Energy Building
PCM	Phase change material
q	Heat flux
r	Radius
TDP	Thermo-diode Panel
s	Surface tension
SA	Stearic acid
TDP	Thermo-diode Panel
TP	Thermosyphon-PCM panel

T	Temperature
TRNSYS	TRaNsient SYStem
R	Thermal Resistance
U	Thermal Conductance
V	Volume

Greek Notations

α	Absorptance
ε	Emissivity
ρ	Density
σ	Stefan-Boltzmann constant
μ	Dynamic/absolute viscosity
∞	Sky

Subscripts

a	Adiabatic section
c	Condenser section
con	Convection
e	Evaporator section
f	Fluid
h	Hydraulic
i	Interior
in	Inside
l	Liquid
o	External
p	Pool
rad	Radiation
sat	Saturation
v	Vapor
hp	Thermosyphon/heat pipe
w	Wall